LAWRENCE
LIVERMORE
NATIONAL
LABORATORY

LLNL-CONF-787820

Self-absorption and Phonon Pulse Shape Discrimination inScintillating Bolometers

G. B. Kim

August 22, 2019

18th International Workshop on Low Temperature Detectors (LTD-18)
Milan, Italy
July 22, 2019 through July 26, 2019

Disclaimer

Journal of Low Temperature Physics manuscript No.
(will be inserted by the editor)

Self-absorption and Phonon Pulse Shape Discrimination in Scintillating Bolometers

Geon-Bo Kim

the date of receipt and acceptance should be inserted later

Abstract We show that self-absorption of photons in scintillating bolometers can differentiate phonon pulse shapes between α (or nuclear recoil) and β/γ signals. This enables phonon pulse shape discrimination for particle identification. We establish a detector signal model that includes self-absorption, and compare the simulated phonon pulse shapes with previously reported experimental results. The model predicts increase of pulse shape difference at higher self-absorption. Base on this result, we propose a new design of scintillating bolometers using 4π light reflectors for maximized self-absorption and only a single phonon readout, instead of light detectors that are typically employed for particle discrimination in scintillating bolometers.

Keywords Scintillating bolometer, cryogenic scintillating calorimeters, pulse shape discrimination, self absorption

1 Introduction

Scintillating bolometers (cryogenic scintillating calorimeters) are employed in rare event detection experiments searching for a dark matter or a neutrinoless double beta decay [1, 2, 3, 4, 5, 6], for their high energy resolution and strong particle identification ability. They simultaneously measure energies that are transferred to phonons (heat) and photons (light) by particle interactions. Interacted particle types can be identified using heat and light amplitude ratios, based on the fact that light yields vary by particle types. α (or nuclear recoil) signals typically exhibit lower light yields than β/γ (electron recoil) signals because of quenching.

In addition, pulse shape discrimination (PSD) technique could be applied to phonon signals that exhibit different pulse shapes between α and β/γ signals [7, 8, 9, 10, 11, 12, 13]. Although the phonon PSD provided excellent discrimination powers, PSD has not been employed as an exclusive method and photon detectors are always installed to guarantee particle identification. This is because the origin that causes pulse shape difference was not

Lawrence Livermore National Laboratory,
Livermore, CA 94550, USA
Tel.:+1-925-422-4232
E-mail: kim90@llnl.gov

fully understood, therefore detectors could not be optimized for phonon PSD for reliable particle identification. For this reason, efforts for improving particle discrimination have been focused on either increasing light collection efficiency or improving the sensitivity of photon detectors [14, 15, 16].

In this paper, we show that the pulse shape differences of phonon signals can be explained by self-absorption of photons in scintillators. Self-absorption produces delayed phonons whose production rate is proportional to the scintillation rate. These delayed phonons contribute to the final phonon signal and slow it down. Different light yields of α and β/γ signals therefore result in different delayed phonon production rates and thus different phonon pulse shapes. A detector signal model is established by taking into account self-absorption and resulting energy flow.

2 Detector Model

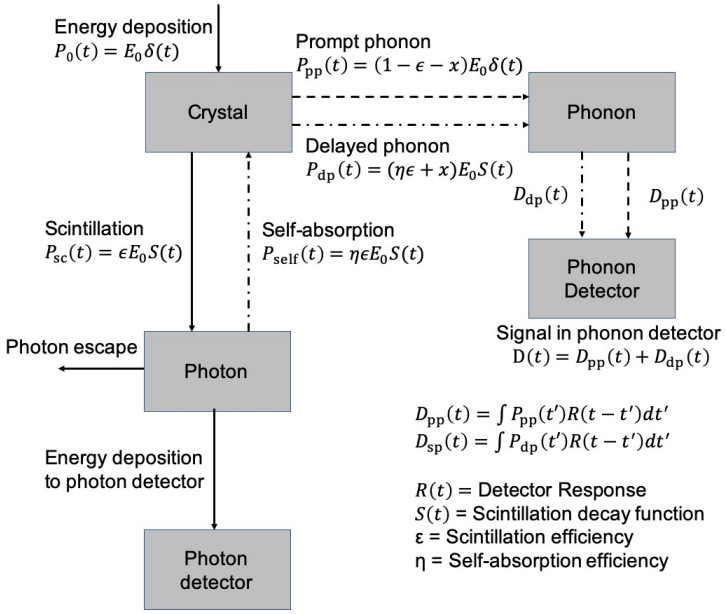

Fig. 1 Schematic diagram of the detector signal model with energy flows (powers) of prompt phonon (*dashed*) and delayed phonon (*dashed-dot*) contributions.

Fig. 1 shows a schematic diagram that describes a detector signal model with self-absorption. Initial energy deposition creates prompt phonons and scintillation photons. A portion of scintillation photons are re-absorbed (self-absorption) to the crystal and produce delayed phonons. Thermal relaxation followed by radiative transition (scintillation) also produces delayed phonons as described in [17]. These prompt and delayed phonons cause a temperature increase of a thermometer (phonon detector). The thermometer response $D(t)$ is determined by thermal resistances and heat capacities of detector components as well as phonon generation rates in the crystal.

The thermometer response to the prompt phonons is expressed as

$$\begin{aligned} D_{\mathrm{pp}}(t) &= \int P_{\mathrm{pp}}(t')R(t-t')dt' \\ &= (1-\varepsilon-x)E_0R(t), \end{aligned} \tag{1}$$

where P_{pp} is prompt phonon production rate, $R(t)$ is detector response that is defined as the thermometer response to instant phonon generation in the detector, ε is scintillation efficiency, x is an energy fraction for post-scintillation thermal relaxation, and E_0 is the total energy deposited to the detector.

The energy transfer rate to scintillation photons can be expressed as

$$P_{\mathrm{sc}}(t) = \varepsilon E_0 S(t), \tag{2}$$

where $S(t)$ is scintillation decay function. A portion of these scintillation photons are self-absorbed to the crystal, and produce delayed phonons. This self-absorption is especially noticeable in heavy inorganic scintillators having high refractive indices (n>1.8), where photons can be trapped inside of the crystal by total internal reflection [18]. The effect of self-absorption is clearly observed in [19].

Energy transfer rate to the delayed phonons can be expressed as

$$P_{\mathrm{dp}}(t) = (\eta\varepsilon + x)E_0 S(t), \tag{3}$$

where η is the self-absorption efficiency that is defined as a fraction of self-absorbed photons to the total number of scintillation photons produced. The timescale of delayed phonon production is same as that of the scintillation.

Post-scintillation thermal relaxation also produces delayed phonons. x is the energy fraction going to this channel. However, it might not be a dominant effect because it cannot explain experimentally observed anti-correlation between light yields and PSD powers shown in 4. x should be proportional to intrinsic light yield, which is opposite to the experimental results. We set the x to 10 % of the total scintillation energy, based on two references [20, 21], although it is an unknown value. Higher x will be preferred for phonon pulse shape discrimination.

The thermometer response to the delayed phonons can be expressed by convoluting the delayed phonon generation rate and detector response.

$$\begin{aligned} D_{\mathrm{dp}}(t) &= \int P_{\mathrm{dp}}(t')R(t-t')dt' \\ &= (\eta\varepsilon + x)E_0 \int S(t')R(t-t')dt'. \end{aligned} \tag{4}$$

A delayed phonon signal, the thermometer response by delayed phonons, will be identical to prompt phonon signals if the scintillation decay is negligibly short compared to the detector response. However, there are scintillators which have very long decay constants at cryogenic temperature, such as $CaMoO_4$ crystals (3.4 ms at 17 mK [22]). Delayed phonon signals in these detectors will be noticeably slower than prompt phonon signals. In our model, we used the whole decay curve including fast and slow components reported in [22].

For signal simulation, a detector response $R(t)$ is generated based on the experimental phonon pulse shape reported in [12] and thermal model equations described in [23, 24]. We assume 10 % intrinsic light yield and 50 % self-absorption efficiency based on [18, 19, 25, 26, 27] for the simulated pulses in fig. 2 and 3. The intrinsic light yield and self-absorption efficiency are adjustable parameters and can be tuned based on future experimental results.

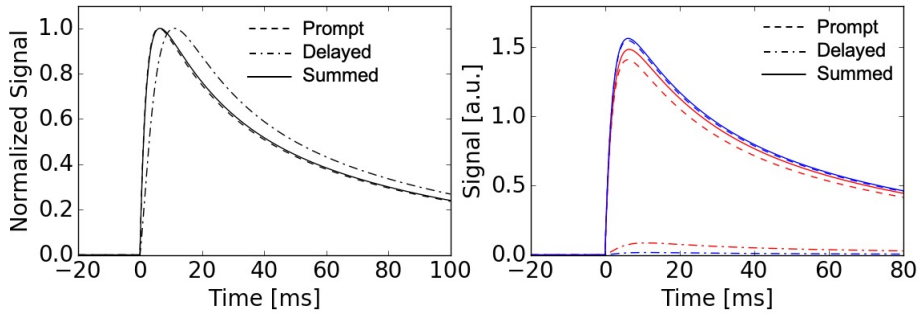

Fig. 2 *Left* Simulated thermometer responses caused by prompt and delayed phonons. Pulses are normalized to their heights for shape comparison. Detector response is generated based on the experimental phonon pulse shape reported in [12]. *Right* Simulated phonon pulse shapes of α (*blue, bigger*) and β/γ (*red, smaller*) signals. Prompt and delayed phonon contributions of each interaction type are compared. (Color figure online.)

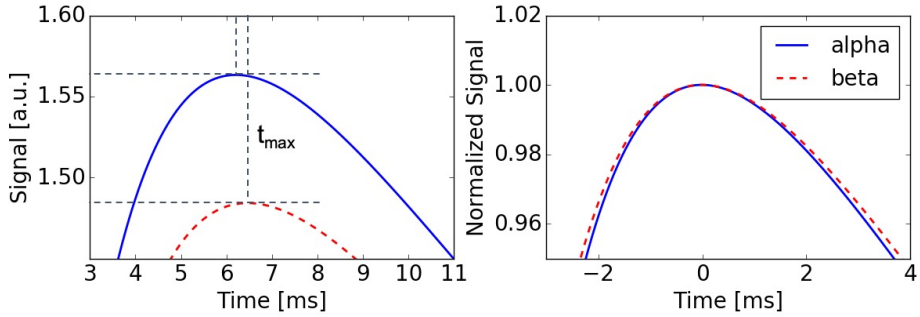

Fig. 3 *Left* Pulse shape comparison at pulse maximum. α signal (*blue, bigger*) is bigger and faster than β/γ signals (*red, smaller*). *Right* α (faster) and β/γ (slower) signals are normalized to their pulse heights and aligned for their pulse maximum times for shape comparison. (Color figure online.)

3 Model Predictions

Self-absorption in scintillating bolometers can result in noticeable features in phonon signals. Our model predicts different phonon pulse shapes between α and β/γ signals, which originates from different light yields and delayed phonon generation. Also, different amplitude scales (different pulse amplitudes for same energy depositions) are expected for α and β/γ signals. We introduce these features and compare with previously reported experimental results.

3.1 Phonon Pulse Shape Differences

Fig. 2 shows simulated prompt and delayed phonon contributions, and summed phonon pulses for α and β/γ signals. Fig. 3 shows phonon signal shapes at their pulse maximums. α signals have lower light yield due to quenching, therefore they have more prompt phonons and less delayed phonons than β/γ signals with higher light yield. As a result, α signals

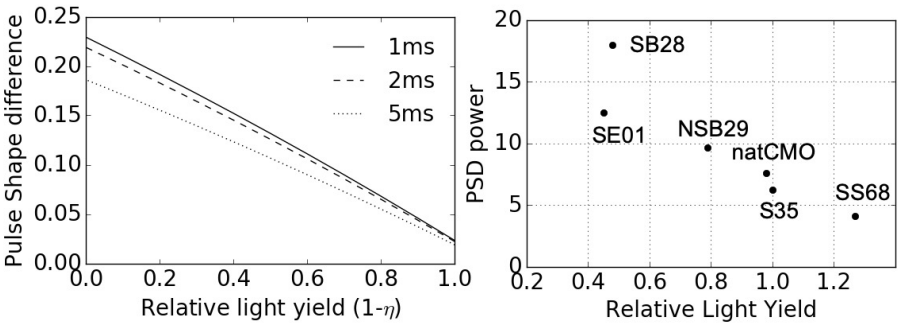

Fig. 4 *Left* Simulated pulse shape differences (pulse meantime) versus relative light yields of scintillating bolometers for different rise-times. *Right* Experimental data for discrimination powers versus measured light yields of $CaMoO_4$ scintillating bolometers reported in [2, 12, 13, 19, 27]. Crystal names in the original publications are labeled.

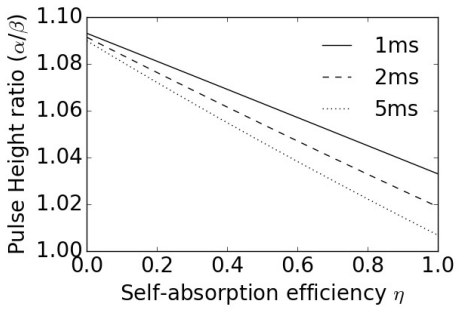

Fig. 5 Simulated pulse height ratios of α and β/γ signals versus self-absorption efficiency. Different rise times are compared.

have bigger pulse heights, and faster rise and decay times than β/γ signals. These model predictions are consistent with experimental observations reported in [12, 13].

Fig. 4 shows simulated pulse shape differences versus relative light yields based on the model. Pulse shape difference is quantified by a meantime parameter that is described in [12]. The model predicts that pulse shape difference will increase as self-absorption increases (that is decrease in light yield). This trend shows good agreement with $CaMoO_4$ experimental data shown in fig. 4. PSD powers and relative light yields are collected from [2, 12, 13, 19, 27].

3.2 Phonon Pulse Amplitude Ratios

Another feature by self-absorption is that α and β/γ phonon signals exhibit different amplitude scales. For the same deposited energy to the detector, α signals have bigger pulse heights than β/γ signals, as shown in fig. 3. This is because α signals have smaller energy loss to scintillation due to their lower scintillation efficiency. However, a portion of the energy loss can be collected via self-absorption. Thus the amplitude ratio of α and β/γ signals varies according to self-absorption efficiency as shown in fig. 5. The amplitude ratio de-

creases as self-absorption increases. If all scintillation photons are re-absorbed, energy loss to scintillation will be zero in both interaction types. However, the amplitude ratio does not converge to 1 because delayed phonon signals with slow rise times do not fully contribute to amplitudes of summed phonon signals.

This amplitude ratio prediction is compared with experimental results of two $CaMoO_4$ scintillating bolometers [12, 13]. These detectors had different transparencies and different self-absorptions [19], and exhibited different amplitude ratios of α and β/γ signals. The "natural CMO" crystal in [13], which had higher light yield and lower self-absorption than the "SB28" crystal in [12], exhibited a bigger amplitude ratio than that of the "SB28" crystal. Their amplitude ratios were approximately 1.07 and 1.03 at 2.6 MeV respectively. The amplitude ratio would not help identifying particle types. However, decreased amplitude ratios in highly self-absorbing detectors are the unique feature that our model predicts. This might help estimating self-absorption efficiency η, if intrinsic light yields are known.

4 Single Phonon Readout Scintillating Bolometer

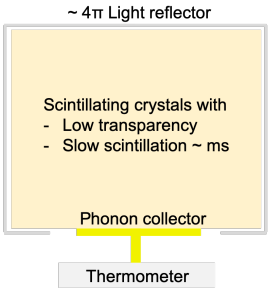

Fig. 6 A proposed scintillating bolometer with a single phonon readout. Instead of using a light detector, a light reflector surrounds the crystal to increase self-absorption.

Separation power Q of pulse shape discrimination can be written as $Q = \delta/\sigma$, where δ is the quantified pulse shape difference (e.g., mean-time or rise-time) and σ is the noise on the pulse shape parameter. Thus, large pulse shape difference and high signal to noise ratio are required to improve particle discrimination power.

Our model suggests that the phonon pulse shape difference can be increased by increasing self-absorption. Based on this prediction, we propose a new scintillating bolometer strategy that uses only a single phonon readout with maximized self-absorption as shown in fig. 5. This is antithetical to typical efforts that minimize self-absorption to improve light yield. 4π light reflectors (with a highly reflective phonon collector made of an Au layer) and low transparency crystals (by omitting annealing procedure that improves transparency) could be considered. This simple detector design eliminates the need for light detectors, which could benefit neutrinoless double beta decay experiments by reducing the number of cryogenic readouts and amplifiers, removing potential background sources of light detector components, and making scaling up of experiments easier.

The proposed detector with high self-absorption could also lower the minimum energy where particle discrimination is applicable, if the signal to noise ratio (SNR), another crucial

factor determining σ is improved together. SNR is mainly determined by thermometer performance (noise and sensitivity), absorber-thermometer coupling, and selection of absorber (phonon physics and heat capacity). These can be improved by independent approaches. For example, there are efforts for lowering the energy threshold of phonon detection, which is being driven for detection of (super-) light dark matters [28, 29] or CENNS [6, 30, 31] of reactor neutrinos, as well as single photon detection in light detectors for particle discrimination [15]. These approaches aim to achieve a few eV or even sub-eV energy thresholds, and will also naturally improve PSD in our proposed detector if they can be adapted to scintillating crystals.

5 Conclusion

Our detector signal model shows that self-absorption can explain phonon pulse shape differences that are observed in scintillating bolometers. The proposed detector with maximized self-absorption could overcome the low light collection efficiency in current scintillating bolometers, therefore improve particle discrimination, as well as simplify detector design that could benefit large scale experiments.

Acknowledgements This work was performed under the auspices of the U.S. DOE by LLNL under Contract DE-AC52-07NA27344

References

1. G. Angloher, et al., The European Physical Journal C **76**(1), 25 (2016). DOI 10.1140/epjc/s10052-016-3877-3
2. V. Alenkov, et al., arXiv preprint arXiv:1903.09483 (2019)
3. D.R. Artusa, et al., The European Physical Journal C **76**(7), 364 (2016). DOI 10.1140/epjc/s10052-016-4223-5
4. M. Tenconi, Physics Procedia **61**, 782 (2015). DOI https://doi.org/10.1016/j.phpro.2014.12.099. 13th International Conference on Topics in Astroparticle and Underground Physics, TAUP 2013
5. I. Bandac, et al., arXiv preprint arXiv:1906.10233 (2019)
6. R. Strauss, et al., The European Physical Journal C **77**(8), 506 (2017). DOI 10.1140/epjc/s10052-017-5068-2
7. L. Gironi, Nucl. Instr. Meth. A **617**(1), 478 (2010). DOI https://doi.org/10.1016/j.nima.2009.10.080. 11th Pisa Meeting on Advanced Detectors
8. C. Arnaboldi, et al., Astroparticle Physics **34**(11), 797 (2011). DOI https://doi.org/10.1016/j.astropartphys.2011.02.006
9. J.W. Beeman, et al., Journal of Instrumentation **8**(05), P05021 (2013). DOI 10.1088/1748-0221/8/05/p05021
10. J.W. Beeman, et al., The European Physical Journal C **72**(9), 2142 (2012). DOI 10.1140/epjc/s10052-012-2142-7
11. J. Beeman, et al., Astroparticle Physics **35**(12), 813 (2012). DOI https://doi.org/10.1016/j.astropartphys.2012.02.013
12. G. Kim, et al., Astroparticle Physics **91**, 105 (2017). DOI https://doi.org/10.1016/j.astropartphys.2017.02.009

13. G.B. Kim, et al., Advances in High Energy Physics **2015**, 817530 (2015). DOI 10.1155/2015/817530
14. J. Rothe, et al., Journal of Low Temperature Physics **193**(5), 1160 (2018). DOI 10.1007/s10909-018-1944-x
15. E. Mondragón, A. Langenkämper, A. Münster, T. Ortmann, L. Pattavina, F. Petricca, W. Potzel, S. Schönert, Nucl. Instr. Meth. A **936**, 182 (2019)
16. N. Casali, et al., Journal of Low Temperature Physics **184**(1), 142 (2016). DOI 10.1007/s10909-015-1358-y
17. L. Gironi, Journal of Low Temperature Physics **167**(3), 504 (2012). DOI 10.1007/s10909-012-0478-x. URL `https://doi.org/10.1007/s10909-012-0478-x`
18. D. Wahl, et al., Nucl. Instr. Meth. A **570**(3), 529 (2007). DOI https://doi.org/10.1016/j.nima.2006.10.099
19. J.H. So, et al., IEEE Transactions on Nuclear Science **59**(5), 2214 (2012). DOI 10.1109/TNS.2012.2200908
20. B. Chandrasekhar, W.B. White, Materials research bulletin **25**(12), 1513 (1990)
21. V. Mikhailik, H. Kraus, M. Itoh, D. Iri, M. Uchida, Journal of Physics: Condensed Matter **17**(46), 7209 (2005)
22. X. Zhang, et al., Applied Physics Letters **106**(24), 241904 (2015)
23. F. Pröbst, et al., Journal of Low Temperature Physics **100**(1), 69 (1995). DOI 10.1007/BF00753837
24. G.B. Kim, et al., Journal of Low Temperature Physics **176**(5), 637 (2014). DOI 10.1007/s10909-014-1139-z
25. V. Mikhailik, H. Kraus, physica status solidi (b) **247**(7), 1583 (2010)
26. A. Annenkov, et al., Nucl. Instr. Meth. A **584**(2-3), 334 (2008)
27. J.Y. Lee, et al., IEEE Transactions on Nuclear Science **63**(2), 543 (2016). DOI 10.1109/TNS.2016.2530828
28. Y. Hochberg, et al., Journal of High Energy Physics **2016**(8), 57 (2016). DOI 10.1007/JHEP08(2016)057
29. S. Knapen, et al., Physics Letters B **785**, 386 (2018). DOI https://doi.org/10.1016/j.physletb.2018.08.064
30. J. Billard, et al., Journal of Physics G: Nuclear and Particle Physics **44**(10), 105101 (2017). DOI 10.1088/1361-6471/aa83d0
31. N. Bastidon, et al., Journal of Low Temperature Physics **193**(5), 1206 (2018). DOI 10.1007/s10909-018-2073-2